Available online at website: https://journal.bcrec.id/index.php/bcrec

Bulletin of Chemical Reaction Engineering & Catalysis, 22 (1) 2027, 42-54

Original Research Article

Biofuel Conversion from Waste Cooking Oil Using Ni-Cu Catalysts Supported on Mesoporous Silica Synthesized via Acidic CTAB-P123 Templating

Ahmad Suseno, Kumala Nadiah Sholika, Yayuk Astuti*

Department of Chemistry, Faculty of Science and Mathematics, Diponegoro University, Tembalang, Semarang, 50275, Indonesia.

Received: 7th September 2026; Revised: 28th October 2026; Accepted: 29th October 2026
Available online: 9th November 2026; Published regularly: April 2027

Abstract

This study investigated the effect of acidic synthesis pH (pH of 1, 3, and 6) on the preparation of mesoporous silica supports for Ni-Cu catalysts used in the hydrocracking of waste cooking oil (WCO) into biofuel. The silica supports were synthesized using a reflux method with CTAB and Pluronic P123 as dual templates, followed by impregnation with 5% Ni-Cu metals at a molar ratio of 3:1. Gas sorption analysis (GSA) revealed that the catalyst synthesized at pH of 6 (K-6) exhibited the highest specific surface area (413.44 m^2/g) and apparent gravimetric ammonia uptake (7.63 mmol/g). X-ray diffraction (XRD) analysis confirmed the amorphous structure of the silica support and the presence of metallic Ni and Cu phases, while Fourier-transform infrared (FTIR) spectroscopy identified characteristic surface hydroxyl and Si-O-Si vibrational bands. Hydrocracking was conducted at a catalyst temperature of 450 °C and a feed vaporization temperature of 500 °C, using a catalyst-to-feed mass ratio of 1:100. Product composition was evaluated using gas chromatography–mass spectrometry (GC-MS). All three catalysts achieved 100% total conversion, with K-6 exhibiting the highest selectivity toward the biofuel fraction (78.99%). These findings highlight the potential of pH-controlled Ni-Cu/mesoporous silica catalysts for biofuel production from WCO and demonstrate the relationship between catalyst textural properties and biofuel selectivity under the investigated reaction conditions.

Copyright © 2027 by Authors, Published by BCREC Publishing Group. This is an open access article under the CC BY-SA License (https://creativecommons.org/licenses/by-sa/4.0).

Keywords: biofuel; catalyst; hydrocracking; mesoporous silica; CTAB; Waste Cooking Oil

How to Cite: Suseno, A., Sholika, K. N., Astuti, Y. (2027). Biofuel Conversion from Waste Cooking Oil Using Ni-Cu Catalysts Supported on Mesoporous Silica Synthesized via Acidic CTAB-P123 Templating. *Bulletin of Chemical Reaction Engineering & Catalysis*, 22 (1), 42-54. (DOI: 10.9767/bcrec.20842)

Permalink/DOI: https://doi.org/10.9767/bcrec.20842

1. Introduction

Global energy demand continues to escalate annually. According to recent data from the International Energy Agency (IEA) in 2023, global energy consumption has exhibited significant growth, driven by sustained economic development and future population increases. Currently, the primary energy supply is derived from fossil fuels, including petroleum, natural gas, and coal [1]. This rising demand has led to a depletion of fossil fuel reserves, necessitating the development of sustainable alternative energy sources. One viable solution is the production of biofuels derived from waste cooking oil (WCO).

Waste cooking oil (WCO) refers to used edible oil generated from cooking processes, which, if disposed of into the environment, leads to water and soil pollution. WCO contains long-chain hydrocarbons, specifically triglyceride compounds, making it a viable feedstock for processing into alternative fuels such as biofuels [2]. The processing of waste cooking oil into biofuel offers a dual solution: reducing reliance on fossil fuels while simultaneously addressing the environmental challenges associated with liquid waste management [3].

The method employed to convert waste cooking oil into biofuel is hydrocracking. Hydrocracking is a process designed to break down large molecules in organic compounds into lighter hydrocarbon fractions with shorter and

* Corresponding Author.
Email: yayuk.astuti@live.undip.ac.id (Y. Astuti)

branched carbon chains [2]. This stage enables the conversion of waste cooking oil into liquid biofuel, which possesses characteristics similar to those of fossil fuels, such as gasoline and diesel. In addition to mitigating reliance on fossil fuels, the utilization of waste cooking oil contributes to the reduction of environmental waste and pollution.

The hydrocracking process can be facilitated by heterogeneous catalysts to break down complex molecular bonds within waste cooking oil and steer the reaction toward the desired products [4]. Transition metal-based catalysts, such as nickel (Ni) and copper (Cu), can form effective bimetallic catalysts for hydrogenation and hydrocarbon cracking processes. Nickel plays an active role in hydrogenation, while copper serves to enhance catalytic selectivity and stability, as well as to minimize agglomeration on the catalyst surface [5]. The activity of these catalysts is highly influenced by the supporting material, or support, which serves to enhance catalytic reactivity.

Mesoporous silica offers significant potential as a catalyst support due to its high specific surface area, which enhances both catalytic reactivity and selectivity [6]. The synthesis of mesoporous silica is influenced by several factors, notably the pH level during the synthesis process. Variations in pH can affect the morphology, pore distribution, and structural stability of the resulting silica material, thereby impacting the catalytic performance in hydrocracking reactions. Previous research on Ni-Cu/mesoporous silica catalysts for hydrocracking of used cooking oil investigated alkaline synthesis conditions at pH 8, 10, and 12, demonstrating that the synthesis pH influenced the textural properties and catalytic performance of the resulting catalysts [7]. These findings highlight the importance of synthesis pH in determining the properties of mesoporous silica and the subsequent catalytic performance. However, the effects of acidic synthesis conditions on the textural properties of mesoporous silica prepared using a CTAB-Pluronic P123 dual-template system, and their implications for Ni-Cu catalyzed hydrocracking of waste cooking oil, require further investigation.

Research regarding the synthesis of mesoporous silica using Pluronic P123 and polystyrene templates, as well as sodium dodecyl sulfate (SDS) surfactants, has been conducted by Siles-Quesada *et al*. [8]. Meléndez-Ortiz *et al.* [9] have also conducted research on the synthesis of mesoporous silica via the hydrothermal method using Pluronic P123 and CTAB templates. Although these studies have demonstrated the feasibility of template-assisted mesoporous silica synthesis, the influence of acidic pH conditions during reflux synthesis using a CTAB-Pluronic P123 dual-template system has not been sufficiently established in the context of Ni-Cu catalyst support development. In particular, understanding how changes in acidic synthesis pH affect the textural properties of the resulting silica and how these properties relate to catalytic performance is important for developing an effective catalyst support.

Accordingly, the novelty of this study lies in the systematic investigation of acidic synthesis pH (pH 1, 3, and 6) during the reflux preparation of mesoporous silica using TEOS as the silica precursor and CTAB-Pluronic P123 as a dual-template system, followed by its application as a support for Ni-Cu catalysts in waste cooking oil hydrocracking. Rather than focusing solely on the preparation method, this study examines the relationship between synthesis pH, the resulting textural properties of mesoporous silica, and the catalytic performance of the supported Ni-Cu catalysts.

This study was conducted to investigate the influence of acidic pH on the synthesis of mesoporous silica as a support for Ni-Cu catalysts in the hydrocracking of waste cooking oil into biofuel. The methodology employed in this research was the reflux method, utilizing TEOS as the silica source and a dual-template system consisting of CTAB and Pluronic P123. Specifically, the study aims to elucidate how variations in acidic synthesis pH affect the textural properties of mesoporous silica and to evaluate how these changes are associated with the catalytic performance of Ni–Cu-supported catalysts in waste cooking oil hydrocracking. The findings are expected to provide insight into the role of synthesis conditions in tailoring mesoporous silica supports for biofuel production.

2. Materials and Methods

2.1. Materials

Tetraethyl orthosilicate (TEOS) (Merck, 98%), cetyltrimethylammonium bromide (CTAB) (Kimia ARD, 99%), pluronic P123 (Merck), Ethanol (Merck, 96%), aquades, aquabides, nickel(II) nitrate hexahydrate ($Ni(NO_3)_2.6H_2O$) (Kimia ARD), copper(II) nitrate trihydrate ($Cu(NO_3)_2.6H_2O$) (Kimia ARD), sodium hydroxide (NaOH) (Merck, 99%), hydrochloric acid (HCl) (Merck, 37%), ammonia (Merck, 25%), waste cooking oil (WCO), hydrogen gas (H_2), and nitrogen gas (N_2).

2.2. Synthesis of Mesoporous Silica Support

The synthesis of mesoporous silica was conducted via the reflux method, with a template-to-silica source ratio of 1:8. Initially, 1 g of Pluronic P123 was dissolved in a mixture of 7.50 mL of deionized water, 5 mL of ethanol, and 15 mL of 2 M HCl. This process was carried out at 35°C with a stirring speed of 400 rpm. Subsequently, 0.10 g of CTAB and 2.70 mL of 98% TEOS were

Copyright © 2027, ISSN 1978-2993

added to the solution and stirred until homogeneous. To achieve the specific pH variations of 1, 3, and 6, 2 M NaOH was added dropwise into the flask. The mixture was then stirred for 5 hours at 35 °C at a speed of 500 rpm.

The resulting homogeneous solution was transferred into a reflux apparatus and heated at 80 °C for 2 hours until a white precipitate formed. The precipitate was separated from the filtrate through filtration and washed with deionized water until a neutral pH was reached. The recovered solids were dried in an oven at 80 °C for 24 hours. The resulting silica powder was ground and sieved through a 200-mesh screen. Finally, the template removal was performed via calcination at 540 °C for 5 hours under a continuous nitrogen (N_2) gas flow.

2.3. Preparation of Ni-Cu/Silica Catalysts via the Impregnation Method

The preparation of Ni-Cu/mesoporous silica catalysts through the impregnation method began by dispersing 2 g of silica in 10 mL of bidistilled water within a beaker. A 5 wt% metal loading was achieved using $Ni(NO_3)_2.6H_2O$ and $Cu(NO_3)_2.3H_2O$ precursor solutions, with a Ni:Cu molar ratio of 3:1. These metal salt solutions were mixed and stirred using a magnetic stirrer until homogeneous. The resulting solution was then added to the silica suspension, and the mixture was agitated using a shaker for 24 hours. Subsequently, the mixture underwent evaporation until all water was removed, followed by drying in an oven for 12 hours. The Ni-Cu/mesoporous silica catalyst was ground into a fine powder and calcined at 500°C for 5 hours under a nitrogen (N_2) atmosphere. The final step involved the reduction of the catalyst under hydrogen (H_2) gas flow at 400°C for 4 hours. The catalysts synthesized at pH 1, 3, and 6 were designated as K-1, K-3, and K-6, respectively.

2.4. Acidity Test of Ni-Cu/Mesoporous Silica Catalysts

The acidity test was conducted using the gravimetric method to determine the total acid site concentration of the Ni-Cu/mesoporous silica catalysts. The procedure began by weighing an empty porcelain crucible, recorded as W1. Subsequently, 0.10 g of the catalyst was placed into the crucible, and the weight was recorded as W2. The crucible containing the catalyst was then placed in a desiccator containing ammonia, which served as the basic adsorbate. This process was carried out for 24 hours within a sealed desiccator. After the adsorption process, the catalyst was weighed again and recorded as W3. The total acidity was then calculated using the following formula:

$$Total\ acidity\ (\text{mmol/g}) = \frac{W_3 - W_2}{(W_2 - W_3) \times \text{MW NH}_3} \times 100 \quad (1)$$

2.5. Characterization of Ni-Cu/Mesoporous Silica Catalysts

The Ni-Cu/mesoporous silica catalysts were characterized using several analytical techniques, namely FTIR (PerkinElmer), XRD (X'Pert^3 Powder), GSA (Nova800), and GC-MS (QP 2010). FTIR analysis was performed in the wavenumber range of 400 to 4000 cm^{-1} to identify the functional groups of the catalyst materials. XRD analysis was conducted to determine the crystallinity of the catalysts and to confirm the presence of active metals. Furthermore, GSA was employed to investigate the physical properties of the catalyst samples, including specific surface area, total pore volume, average pore size, and pore size distribution.

2.6. Activity and Selectivity Testing of Ni-Cu/Mesoporous Silica Catalysts in Hydrocracking Reactions

Figure 1 illustrates the reactor setup used for the hydrocracking of waste cooking oil (WCO) into biofuel using Ni-Cu/mesoporous silica catalysts. In this hydrocracking process, the catalyst-to-feed ratio was maintained at 1:100. The cracking process was initiated by loading 0.20 g of the catalyst into the reactor column and heating it to 450 °C. The catalytic activity was evaluated by

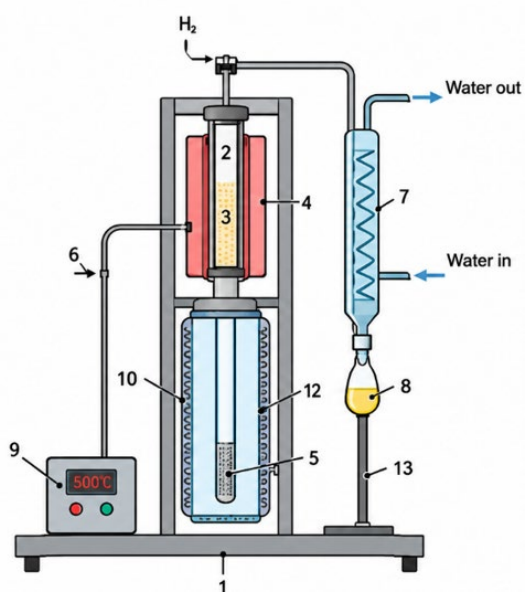


Figure 1. Hydrocracking reactor setup. (1). Frame, (2). Feed reactor, (3). Catalytic reactor, (4). Feed holder/chamber, (5). Catalyst holder/bed, (6). Gas inlet, (7). Condenser, (8). Product collector/receiver, (9). Temperature controller, (10). Temperature sensor / Thermocouple, (11). Hinge, (12). Hook/Latch, (13). Retort stand / Support stand.

Copyright © 2027, ISSN 1978-2993

introducing 20 g of WCO as the feedstock into the evaporator column, which was preheated to 500 °C. The reaction proceeded for 1 hour under a continuous hydrogen (H_2) gas flow at a rate of 20 mL/min.

The resulting liquid products were analyzed using Gas Chromatography-Mass Spectrometry (GC-MS) to identify the chemical compounds formed. The catalytic activity and selectivity in the hydrocracking reaction were calculated using the following equations:

$$Liquid\ prod.yield\ (\%) = \frac{W_{LP}}{W_F} \times 100\% \quad (2)$$

$$Solid\ prod.yield\ (\%) = \frac{W_R + (W_{UC} - W_{FC})}{W_F} \times 100\% \quad (3)$$

$$Gas\ prod.\ yield\ (\%) = 100\% - (liquid\ prod.\ yield - solid\ prod.\ yield) \quad (4)$$

$$Catalytic\ activity\ (\%) = liquid\ product + solid\ product + gas\ product \quad (5)$$

$$Selectivity\ to\ target\ compound\ (\%) = \frac{\%\ area\ of\ target\ compound}{\%\ total\ area\ in\ GCMS} \times 100\% \quad (6)$$

where, W_{LP} is weight of liquid product (g), W_F is weight of feedstock (WCO) (g), W_R is weight of residue (g), W_{FC} is weight of fresh catalyst (g), and W_{UC} is weight of used catalyst (g).

3. Results and Discussion

3.1. Mesoporous Silica Support

The synthesis of mesoporous silica aims to produce silica with a high specific surface area and a mesoporous structure (2–50 nm). Silica with a high surface area provides a greater number of active sites, making it an ideal support for hydrocracking reactions. This material plays a crucial role in ensuring a uniform catalyst distribution, enhancing reactant accessibility to the active sites, and accelerating the reaction rate. Mesoporous silica was synthesized using TEOS as the silica source, combined with CTAB and Pluronic P123 as templates to direct the formation of the porous structure. The use of CTAB functions as a pore-directing agent for small mesopores (1–3 nm), while Pluronic P123 facilitates the formation of larger (4–10 nm) and more ordered pores. The combination of these two templates enables the development of a mesoporous structure with diverse pore sizes and enhanced thermal stability.

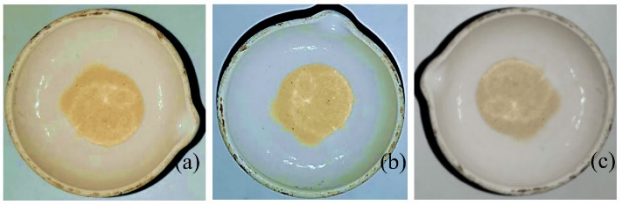


Figure 2. Synthesized mesoporous silica at (a) pH of 1, (b) pH of 3, and (c) pH of 6.

The synthesis process was conducted under acidic conditions with the addition of HCl to accelerate the hydrolysis process, yield more stable functional groups, and facilitate the removal of leaving groups [10]. The synthesis of mesoporous silica involves hydrolysis and condensation reactions. Under acidic conditions, the hydrolysis reaction begins with the protonation of alkoxy groups (–OR) on the silica structure such as ≡Si–O^- (anionic siloxide), ≡Si–OH (silanol), and ≡Si–OR (alkoxysilane) by H^+ ions. This protonation generates a highly electrophilic ≡Si–O^+HR group, which is susceptible to nucleophilic attack by water molecules. Subsequently, the silicon atom undergoes nucleophilic attack by water, resulting in the formation of a pentacoordinate intermediate structure. Once the intermediate is formed, the alkoxy group is displaced as an alcohol molecule (ROH), leading to the formation of silanol groups (Si–OH).

The condensation reaction begins with the protonation of the hydroxyl group (–OH) on the silanol molecule by H^+ ions under acidic conditions, producing a more electrophilic –OH_2^+ group. Subsequently, the silanol molecules undergo polymerization; the –OH group acts as a nucleophile, attacking the protonated electrophilic Si center. This reaction results in the formation of siloxane groups (Si–O–Si). The synthesized silica is then calcined at 540 °C under a nitrogen gas flow for 5 hours to remove the Pluronic P123 and CTAB templates, thereby generating the porous silica structure. The resulting silica supports are obtained as brownish-yellow powders, as shown in Figure 2. Silica synthesized at pH of 1 and pH of 3 exhibits a coarse texture and low volume, whereas silica synthesized at pH of 6 shows a finer texture and higher volume. These variations in pH significantly influence the hydrolysis and condensation rates during the synthesis process.

Under strongly acidic conditions (low pH), the hydrolysis reaction proceeds rapidly, yielding an abundance of silica precursors (Si–OH); however, the condensation rate remains slow. This slow condensation rate results in silica with a denser and coarser texture due to limited particle agglomeration. Conversely, at a higher pH, the condensation rate increases, thereby accelerating the formation of the siloxane network (Si–O–Si). The increased condensation rate leads to a larger pore volume and a finer texture, resulting from the formation of looser and less compact particle aggregates.

Copyright © 2027, ISSN 1978-2993

3.2. Ni-Cu/Mesoporous Silica Catalysts

The Ni-Cu/mesoporous silica catalysts were prepared using the wet impregnation method. This method aims to incorporate Ni and Cu metals, which serve as the active catalytic components, into the pores of the mesoporous silica that acts as the support. Wet impregnation is performed by immersing the silica in a metal salt solution with a volume exceeding the total pore volume of the support [11]. The Ni and Cu metals were impregnated into the silica powder with a molar ratio of 3:1. This specific ratio was selected to enhance the catalytic activity during the hydrocracking reaction by prioritizing Ni as the primary active phase. Meanwhile, the addition of Cu as a promoter functions to prevent metal agglomeration and improve the distribution of Ni species across the silica support surface [5]. The combination of Ni and Cu has also been reported to enhance the catalytic performance of mesoporous silica-supported catalysts through synergistic effects associated with hydrogen activation, active-site enhancement, and selective C-C bond cleavage during hydrocracking [12].

Calcination and reduction are crucial stages in the synthesis of transition metal catalysts following the impregnation process. Calcination was performed at 500 °C for 5 hours under an inert nitrogen (N_2) atmosphere. The primary objectives of calcination are to eliminate organic impurities, such as residual solvents, and to remove nitrates by decomposing NO_3^- ions originating from the $Ni(NO)_3.6H_2O$ salt [13]. Furthermore, conducting calcination prior to reduction can enhance the dispersion of Ni and Cu species. The final stage involves reducing the sample using hydrogen (H_2) gas at 400 °C for 4 hours. The purpose of this reduction is to transform metal oxides into their metallic active forms (Ni and Cu), thereby increasing the catalytic activity of the material [13]. The reaction mechanisms for the formation of metallic Ni and Cu are as follows [14]:

$$Ni(NO_3)_2.6H_2O_{(s)} \rightarrow Ni(NO_3)_{2(s)} + 6H_2O_{(g)} \quad (6)$$
$$2Ni(NO_3)_{2(s)} \rightarrow 2NiO_{(s)} + 4NO_{2(g)} + O_{2(g)} \quad (7)$$
$$NiO_{(s)} + H_{2(g)} \rightarrow Ni_{(s)} + H_2O_{(g)} \quad (8)$$
$$Cu(NO_3)_2.3H_2O_{(s)} \rightarrow Cu(NO_3)_{2(s)} + 3H_2O_{(g)} \quad (9)$$

Table 1. Textural properties of the synthesized catalysts.

Catalyst	Specific Surface Area (m^2/g)	Pore Volume (cm^3/g)	Avarage Pore Diameter (nm)
K-1	62.96	0.28	17.94
K-3	46.44	0.13	11.33
K-6	413.44	1.02	9.86

$$2Cu(NO_3)_{2(s)} \rightarrow 2CuO_{(s)} + 4NO_{2(g)} + O_{2(g)} \quad (10)$$
$$CuO_{(s)} + H_{2(g)} \rightarrow Cu_{(s)} + H_2O_{(g)} \quad (11)$$

The synthesized Ni-Cu/mesoporous silica catalysts specifically the K-1, K-3, and K-6 variants exhibited a color transition from the initial brownish-yellow to dark brown. This color change indicates that the metal oxides (NiO and CuO) have been successfully reduced into metallic Ni and Cu. The Ni-Cu-based catalysts increase the number of active sites on the surface, thereby enhancing the catalytic reaction rate. The presence of silanol groups (Si–OH) on the silica provides Brønsted acid sites that act as proton (H^+) donors. Meanwhile, the Ni and Cu metals possess vacant orbitals, functioning as Lewis acid sites by accepting electron pairs. The interaction between the metals and the silica support forms coordinate covalent bonds, where the metal acts as the central atom and the silica serves as the electron-donating ligand.

3.3. Surface Area and Porosity Characteristics of the Catalysts

Surface analysis was conducted to understand the physical properties of the Ni-Cu/mesoporous silica catalysts for the K-1, K-3, and K-6 variants. The characterization was performed using a Gas Sorption Analysis (GSA) instrument, which includes the determination of the specific surface area, pore volume, and average pore size via the Brunauer–Emmett–Teller (BET) method. Additionally, the pore size distribution was analyzed using the Barrett-Joyner-Halenda (BJH) method.

Table 1 presents the textural properties of the K-1, K-3, and K-6 catalysts based on the BET analysis results. The data reveals that the K-6 catalyst exhibits the highest specific surface area at 413.44 m^2/g, followed by K-1 (62.96 m^2/g) and K-3 (46.44 m^2/g). The significantly higher surface area of K-6 is attributed to its smaller pore diameter of 9.86 nm and a high pore volume of 1.02 cm^3/g. These values indicate that the porous structure formed under weak acidic conditions (pH of 6) provides greater accessibility to active sites for catalytic reactions, consistent with the importance of textural properties and active-site accessibility in supported metal catalysts [15]. Conversely, at lower pH levels (pH of 1 and 3), the hydrolysis of the silica precursor (TEOS) proceeds rapidly, but the condensation rate remains slow. This kinetic imbalance leads to the formation of larger silica particles with larger average pore diameters but lower pore density [16].

Figure 3 displays the nitrogen adsorption-desorption isotherm curves for the K-1, K-3, and K-6 catalysts. These graphs illustrate the relationship between the amount of nitrogen gas adsorbed and desorbed at Standard Temperature

Copyright © 2027, ISSN 1978-2993

and Pressure (STP) against the relative pressure (P/P_0) at a constant temperature. According to the IUPAC classification, all three catalysts exhibit Type IV isotherms, which signify that the materials are mesoporous with pore sizes ranging from 2 to 50 nm. Similar nitrogen adsorption-desorption behavior has been reported for CTAB-templated mesoporous silica materials [17]. This isotherm type is characterized by a step-like curve, representing a gradual multilayer adsorption process.

According to the IUPAC classification for hysteresis loops, all three catalysts exhibit Type H1 behavior, which indicates a high degree of pore size uniformity. This is evidenced by the narrow and symmetrical shape of the hysteresis loops between the adsorption and desorption branches. Type H1 hysteresis is characterized by nearly parallel and sharp adsorption and desorption isotherms [16]. The K-6 catalyst displays a broader hysteresis range compared to the other variants; this is attributed to an increase in the total pore volume, which subsequently leads to a greater adsorption capacity.

Figure 4 presents the pore size distribution curves obtained using the Barrett–Joyner–Halenda (BJH) method for the K-1, K-3, and K-6 catalyst samples. Based on the plots, all three catalysts are confirmed to be mesoporous materials. The K-1 and K-3 catalysts exhibit pore size distributions with dominant peaks at diameters of 8–10 nm, with dV(r) values of 0.028 cm^3/Å/g for K-1 and 0.022 cm^3/Å/g for K-3, respectively. Synthesis at low pH (1 and 3) tends to form uniform small pores due to the slow condensation process. Increasing the synthesis pH for the K-6 catalyst resulted in a significant structural transformation, marked by a much higher dV(r) peak reaching 0.25 cm^3/Å/g. The K-6 catalyst exhibits a dominant pore diameter between 5 and 8 nm with a narrow distribution peak. This indicates that the K-6 catalyst possesses a more specific and uniform pore size distribution compared to the K-1 and K-3 catalysts.

3.4. Gravimetric Ammonia Adsorption Analysis

Acidity testing was conducted to determine the total acidity using the gravimetric method. This method is based on the weight difference of the catalyst before and after the adsorption of ammonia (NH_3) as a basic probe molecule onto the acid sites on the silica catalyst surface. The mass increase provides a quantitative basis for comparing the apparent ammonia uptake of the catalysts under identical experimental conditions. This approach offers a practical means of evaluating differences in ammonia adsorption among the catalyst samples, which can be considered alongside their textural properties and catalytic performance. The results therefore provide complementary information for understanding the characteristics of the Ni–Cu/mesoporous silica catalysts. The acid sites on

Table 2. Apparent gravimetric ammonia uptake.

Catalyst Sample	Acidity (mmol/g)
K-1	6.47
K-3	5.90
K-6	7.63

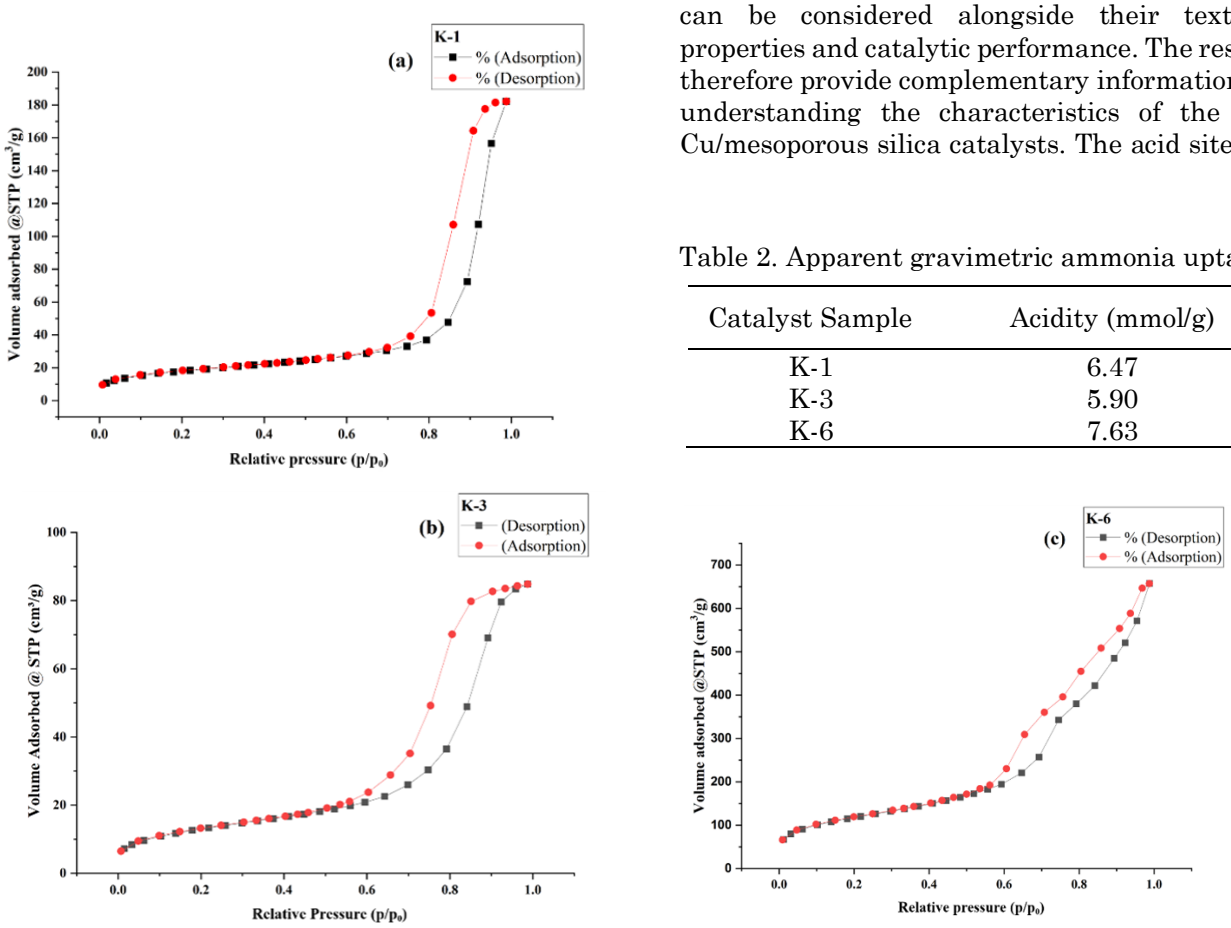


Figure 3. Nitrogen adsorption-desorption isotherms of catalysts (a) K-1, (b) K-3, and (c) K-6.

Copyright © 2027, ISSN 1978-2993

the catalyst possess the capability to adsorb NH_3; specifically, Brønsted acid sites release H^+ ions to form NH_4^+, which is then adsorbed by the catalyst [18].

Table 2 shows that the highest apparent ammonia uptake is observed in the K-6 catalyst at 7.63 mmol/g, followed by K-1 at 6.47 mmol/g and K-3 at 5.90 mmol/g. These results indicate that K-6 exhibits the highest ammonia uptake among the investigated catalysts under the applied experimental conditions. The superior surface area of the K-6 catalyst provides a larger surface area potentially accessible for ammonia adsorption, which may contribute to the observed uptake. The differences in ammonia uptake reflect variations in the adsorption characteristics of the catalysts and provide complementary information for evaluating their surface properties. The availability of accessible surface sites for ammonia adsorption is an important characteristic in catalyst evaluation and can be considered alongside other physicochemical properties when discussing catalytic performance. In this study, K-6 exhibited both the highest apparent ammonia uptake and the largest specific surface area, making it a promising catalyst among the samples investigated.

3.5. Functional Group Composition of the Catalysts

Functional group analysis aims to identify the presence of chemical groups on the catalyst surface following the gravimetric process, based on Fourier-Transform Infrared (FTIR) spectra. Furthermore, FTIR characterization is employed to detect the absorption bands associated with surface functional groups and to explore spectral features that may be related to the acid properties of the K-1, K-3, and K-6 catalyst samples. The wavenumbers used to measure the absorption bands of the catalysts range from 400 to 4000 cm^{-1}.

Figure 5 illustrates that all three catalyst samples (K-1, K-3, and K-6) exhibit functional group characteristics typical of silica-based materials. The siloxane (Si–O–Si) groups are identified by sharp peaks in the wavenumber range of 1047–1060 cm^{-1}, corresponding to asymmetric stretching vibrations, and at 790–795 cm^{-1}, corresponding to symmetric stretching vibrations [19]. The hydroxyl groups (Si–OH) are indicated by the peaks at the wavenumber of 3375 cm^{-1}, which correspond to the O–H stretching vibrations [20]. The presence of adsorbed water is indicated by the peaks at wavenumbers 1634–1629 cm^{-1}, which correspond to the –OH bending vibrations [19]. A more detailed interpretation of the FTIR results for each catalyst sample is presented in Table 3.

The presence of acid groups was indicated by the -OH group signals, suggesting the existence of N–H vibrations from ammonia interacting with the silanol groups [21]. However, significant peak overlapping occurred in this region, necessitating peak deconvolution using Fityk software to resolve the individual contributions. The deconvolution results were used to facilitate the interpretation of overlapping bands, while the assignment of specific acid-site types was

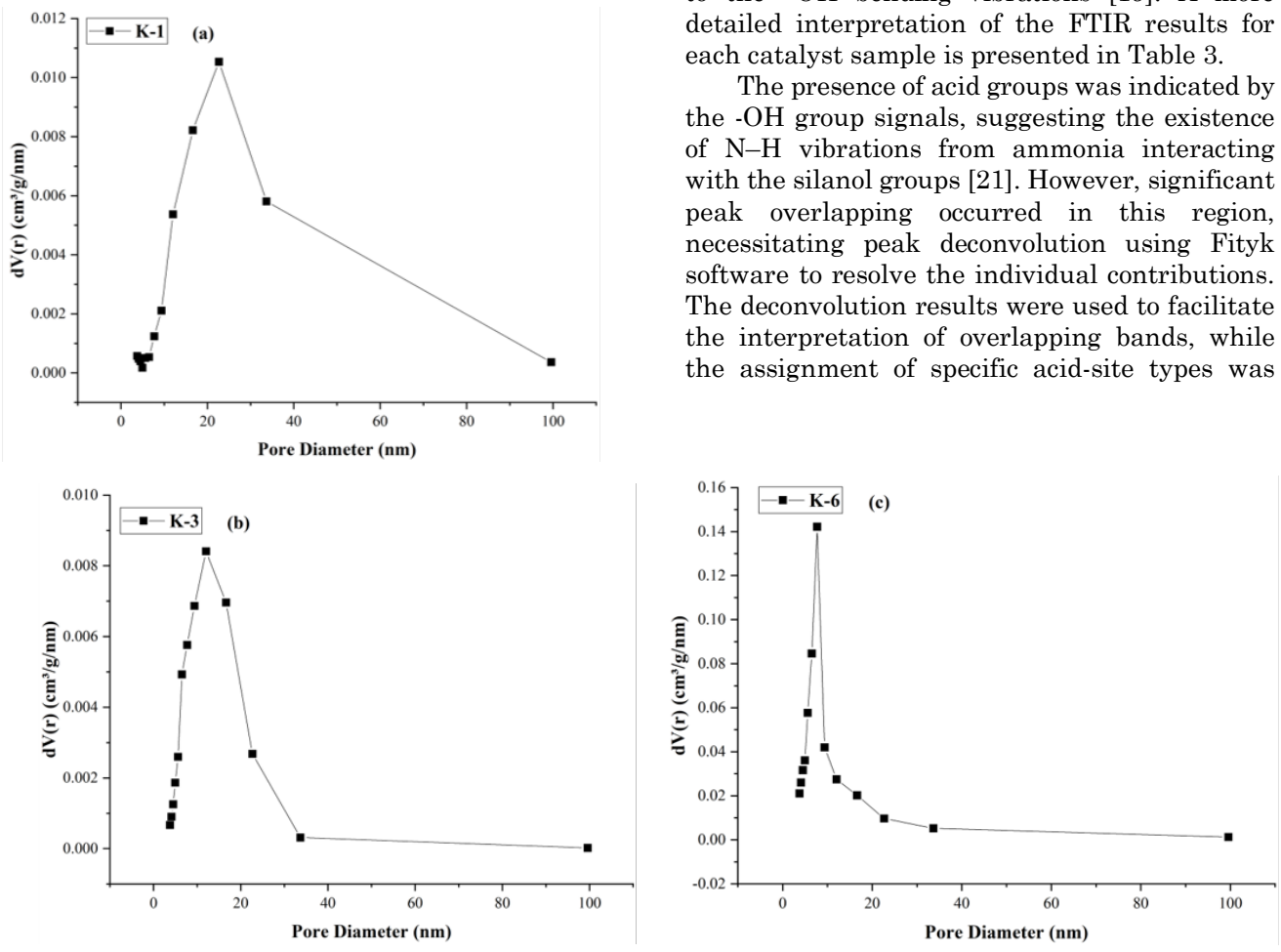


Figure 4. Pore size distribution curves of (a) K-1, (b) K-3, and (c) K-6.

Copyright © 2027, ISSN 1978-2993

considered in view of the limitations of the FTIR measurements performed in this study.

Figure 6 illustrates the FTIR deconvolution results for the K-1, K-3, and K-6 catalyst samples. The results reveal two dominant fitted peaks.The bands associated with the bending vibration of adsorbed water were observed at wavenumbers of 1633.10 cm^{-1} for K-1, 1633.93 cm^{-1} for K-3, and 1633.64 cm^{-1} for K-6. These spectral features may be related to interactions between the transition metal centers (Ni and Cu) and ammonia molecules. The transition metals act as electron acceptors due to their vacant d-orbitals, enabling them to accept lone pair electrons from ammonia. Consequently, ammonia acts as an electron donor, forming coordination bonds with the metals.

The surface-related vibrational bands for K-1, K-3, and K-6 were observed at wavenumbers of 1458.60 cm^{-1}, 1457.32 cm^{-1}, and 1457.82 cm^{-1}, respectively. These spectral features may be related to interactions between ammonia and proton-donating hydroxyl (-OH) groups on the silica surface. Such interactions may involve proton transfer from surface hydroxyl groups to ammonia, resulting in the formation of ammonium ions (NH_4^+). Brønsted acid sites are generally considered important in acid-catalyzed reactions involving the activation of substrate molecules, such as triglycerides. Such acid-catalyzed pathways may facilitate the conversion of triglycerides into shorter-chain hydrocarbon fractions through bond cleavage reactions, including those involving C-O and C-C bonds.

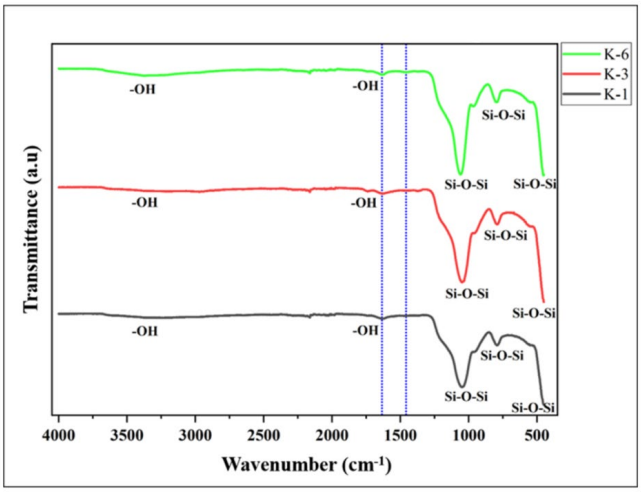


Figure 5. FTIR spectra of the catalysts after acidity testing.

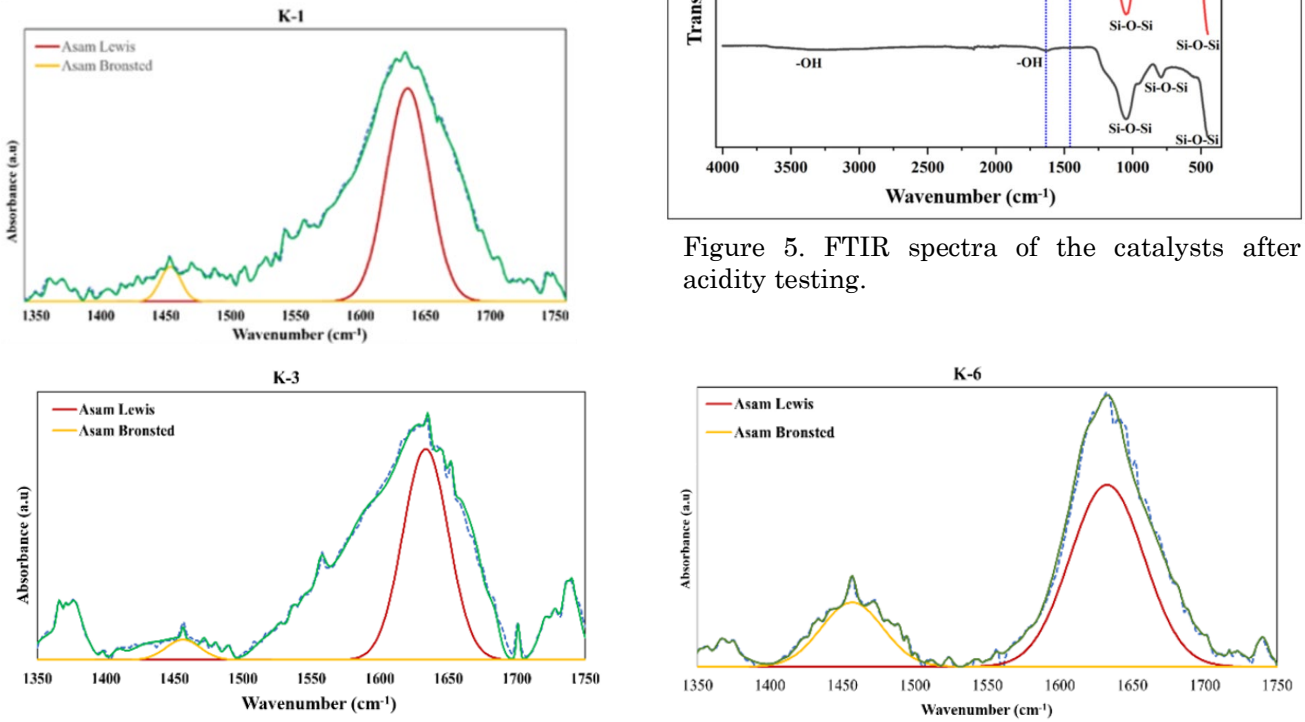


Figure 6. FTIR deconvolution results for (a) K-1, (b) K-3, and (c) K-6 samples.

Table 3. Interpretation of FTIR spectra.

Wavenumber (cm^{-1})			Interpretation
K-1	K-3	K-6	
3375.82	3375.82	3375.82	Stretching vibration of -OH from silanol groups (Si-OH)
1633.13	1633.92	1633.62	O-H bending vibration
1624.72	1624.82	1621.35	Bending vibration of -OH from Si-OH
1458.62	1457.33	1457.85	Surface-related vibrational band
1047.20	1048.73	1060.24	Asymmetric stretching vibration of Si–O from Si-O-Si
790.25	787.95	795.62	Symmetric stretching vibration of Si–O from Si-O-Si
451.24	452.01	451.24	Bending vibration of Si-O-Si

Copyright © 2027, ISSN 1978-2993

3.6. Catalyst Crystallinity

Catalyst crystallinity is a critical parameter that influences the specific surface area, phase distribution, and the interaction between active metals and their support. The X-Ray Diffraction (XRD) analysis analysis aims to investigate the effect of pH on the resulting silica catalyst structure and to determine the presence of active metals, specifically Ni and Cu, following the reduction of NiO and CuO.

Figure 7 displays the XRD diffractograms of the three catalyst samples K-1, K-3, and K-6. Based on the data, all three samples exhibit the characteristic pattern of amorphous silica (SiO_2) identified by a broad peak at 2θ = 23° [19]. The broadening of this peak is attributed to the long-range disorder in the atomic structure, which causes the reflected X-ray waves to scatter more randomly. The presence of metallic Cu is identified by peaks at 2θ = 43.32° and 50.44° (ICDD No. 00-003-1018). Metallic Ni is observed at 2θ = 44.48° (ICDD No. 00-004-085). Furthermore, metal oxide phases are still detectable at 2θ = 38.8° for NiO (ICDD No.00-004-0835) and 38.70° for CuO (ICDD No. 00-048-1548). The presence of these metal oxides indicates that the reduction process was not entirely complete, leaving a portion of the metals in their oxidized states [22].

3.6. Catalytic Activity and Selectivity in the Hydrocracking Process

The evaluation of catalytic activity and selectivity in hydrocracking applications is a critical stage in determining the catalyst's capability to convert waste cooking oil (WCO) into biofuel. Waste cooking oil has also been investigated as a feedstock for catalytic deoxygenation to produce renewable hydrocarbon fuels, demonstrating the potential of Ni-based catalysts for WCO conversion [23]. Hydrocracking is a cracking process employed to transform long-chain hydrocarbon compounds into lighter fractions [24]. Catalytic activity is assessed by the catalyst's ability to convert a specific amount of waste cooking oil feedstock into biofuel products, whereas selectivity refers to the catalyst's proficiency in producing specific product types based on GC-MS (Gas Chromatography-Mass Spectrometry) analysis.

The hydrocracking process was conducted using a weight ratio of 1:100 between the catalyst and waste cooking oil. Twenty grams of waste cooking oil and 0.2 g of catalyst were utilized; the catalyst was heated to 450 °C, while the oil vaporization was maintained at 500 °C for 1 hour. The reaction proceeded under a continuous flow of nitrogen (N_2) gas to prevent contact with oxygen, transport the oil vapor to the condenser, and inhibit the formation of by-products such as H_2O, CO, and CO_2 [25].

Table 4 presents the results of the catalytic activity and selectivity tests for the hydrocracking of waste cooking oil into biofuel, conducted using two methods: thermal cracking and catalytic cracking. The results indicate that hydrocracking using a catalyst yields a significantly higher biofuel conversion compared to thermal hydrocracking. The thermal treatment produced a total biofuel yield of 44.64%, whereas the use of catalysts K-1, K-3, and K-6 resulted in total biofuel yields of 70.85%, 70.23%, and 78.99%, respectively. Catalyst K-6 exhibited the highest total biofuel conversion, with a dominant distribution in the C_{16}-C_{18} range,

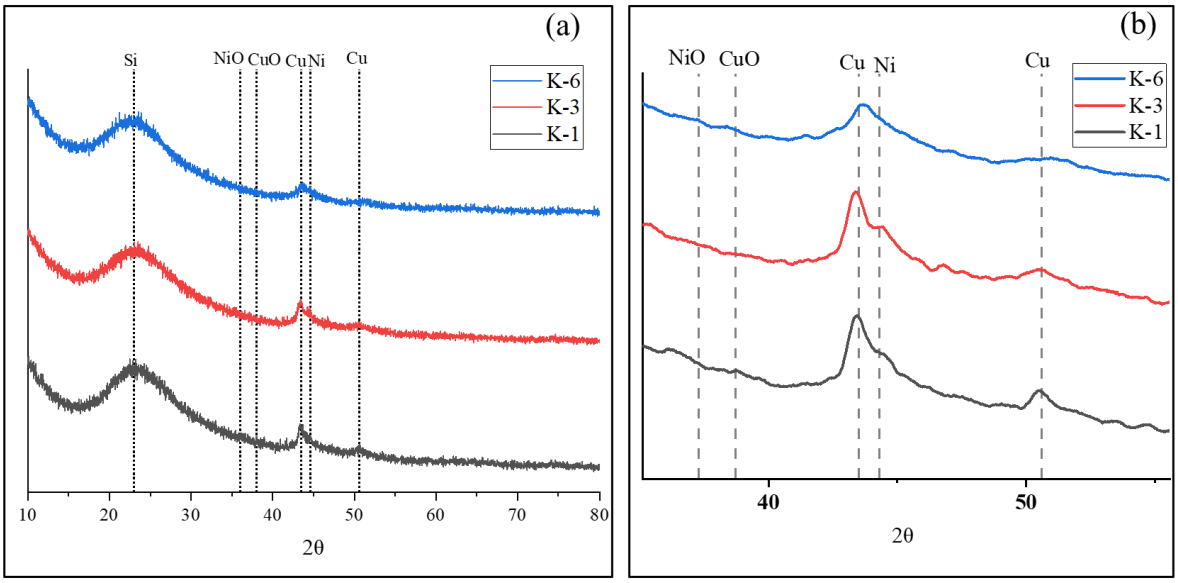


Figure 7. XRD diffractograms: (a) full-scale pattern and (b) magnified view.

Copyright © 2027, ISSN 1978-2993

which falls within the biodiesel fraction. This performance is supported by its large specific surface area of 413.45 m^2/g, a pore volume of 1.02 cm^3/g, and an average pore diameter of 9.86 nm, all of which are characteristic of mesoporous silica materials. The mesoporous structure facilitates the diffusion of large molecules, such as triglycerides in waste cooking oil, into the pores, thereby providing better access to the active sites on the catalyst surface. In contrast, catalysts K-1 and K-3 showed lower total biofuel yields compared to K-6. This lower activity is attributed to their significantly smaller surface areas, recorded at 62.96 m^2/g for K-1 and 46.44 m^2/g for K-3. Furthermore, the pore volumes for these catalysts were also lower than K-6, at 0.28 cm^3/g for K-1 and 0.13 cm^3/g for K-3. The limited surface area and pore volume restrict the access of reactant molecules to the catalyst's active sites, consequently resulting in lower total biofuel conversion.

Figure 8 illustrates the relationship between catalyst acidity and selectivity. The obtained data reveal a linear correlation between the acidity of the catalyst and the total selectivity toward the produced biofuel. An increase in the catalyst's acidity value leads to higher selectivity toward the biofuel fraction. Catalyst K-6 possessed the highest acidity value at 7.63 mmol/g, resulting in higher selectivity for the biofuel fraction compared to K-1 and K-3. High acidity values indicate a greater abundance of both Brønsted and Lewis acid sites. These acid sites play a pivotal role in the cleavage of C-C and C-O bonds within triglyceride molecules during the hydrocracking of waste cooking oil.

Figure 9 presents the percentage of biofuel product generated through the hydrocracking reaction using catalysts K-1, K-3, and K-6. Catalyst K-1 yielded a product composition of olefins (56.94%), paraffins (31.23%), cyclics (11.6%), and aromatics (0.23%). Catalyst K-3 produced olefins (61.87%), paraffins (29.64%), cyclics (6.62%), and aromatics (1.87%). Meanwhile, catalyst K-6 produced paraffins (55.72%), olefins (41.21%), and cyclics (3.07%). The primary product from the hydrocracking reactions using K-1 and K-3 was olefins, whereas K-6 predominantly produced paraffins. The formation of hydrocarbon-based products from waste cooking oil is consistent with previous studies employing Ni/mesoporous silica catalysts, which demonstrated the capability of Ni-based mesoporous catalysts to promote the deoxygenation of oxygen-containing compounds in waste cooking oil [26]. This indicates that catalyst K-6 exhibits the most optimal performance in waste cooking oil conversion, characterized by the dominance of paraffinic products. The specific pore diameter of K-6 (9.86 nm) optimizes hydrogen adsorption and enhances the interaction between the Ni–Cu active sites and hydrocarbons during the hydrogenation reaction. Furthermore, larger molecules undergo extensive cracking to produce smaller, saturated compounds, which can subsequently diffuse out of the pores.

Overall, the results demonstrate that the synthesis pH influences the textural characteristics and hydrocracking performance of the Ni-Cu catalysts supported on mesoporous silica. Among the investigated samples, K-6 showed the highest thermal activity (78.99%), compared with K-1 (70.85%) and K-3 (70.23%). These findings support the objective of evaluating synthesis pH as a factor affecting catalyst properties and performance under the experimental conditions employed.

4. Conclusion

Ni-Cu/mesoporous silica catalysts were successfully synthesized using a reflux method with a CTAB-Pluronic P123 dual-template system at different acidic synthesis pH values (pH 1, 3, and 6). Among the investigated catalysts, K-6 exhibited the highest specific surface area (413.44 m^2/g) and apparent gravimetric ammonia uptake (7.63 mmol/g), followed by K-1 (62.96 m^2/g and 6.47 mmol/g) and K-3 (46.44 m^2/g and 5.90 mmol/g). XRD analysis confirmed the amorphous structure of the silica support and the presence of metallic Ni and Cu phases, while FTIR analysis revealed characteristic surface hydroxyl and Si-O-Si

Table 4. Percentage of selectivity and catalytic activity for biofuel fractions.

Treatment	Biofuel Selectivity			Total Biofuel Yield	Non-biofuel	Biofuel Activity
	C_5-C_{12}	C_{13}-C_{15}	C_{16}-C_{18}	(%)	$>C_{18}$ (%)	(%)
Thermal	20.50	16.32	18.53	55.36	44.64	-
K-1	28.76	10.78	31.31	70.85	29.19	100
K-3	24.65	15.05	30.53	70.23	29.80	100
K-6	18.25	9.26	51.48	78.99	21.00	100

Copyright © 2027, ISSN 1978-2993

vibrational bands. The catalysts demonstrated higher biofuel fraction selectivity than thermal hydrocracking under the investigated conditions. All three catalysts achieved 100% total conversion, with K-6 exhibiting the highest biofuel selectivity of 78.99%. The superior textural properties of K-6, particularly its specific surface area of 413.44 m^2/g, may contribute to the accessibility of reactants to the catalyst surface and the observed biofuel selectivity. These findings demonstrate the applicability of the reflux-assisted CTAB-Pluronic P123 dual-template approach for preparing mesoporous silica supports under acidic conditions and highlight the relationship between the resulting catalyst properties and biofuel selectivity. In particular, K-6 exhibited the highest specific surface area and biofuel selectivity among the catalysts investigated. This study therefore provides experimental insight into the development of Ni-Cu/mesoporous silica catalysts for waste cooking oil hydrocracking under the investigated conditions.

Acknowledgements

The authors would like to thank the Faculty of Science and Mathematics, Diponegoro University for supporting this research with grant number 30.E/UN7.F8/PP/II/2026 for the 2026 fiscal year.

Conflict of Interest Statement

The authors declare that there are no financial or personal relationships that could be perceived as influencing the research presented in this manuscript.

Declaration of Generative AI Use

Generative AI was used to redraw Figure 1. The revised figure was reviewed and verified by the authors to ensure its accuracy and consistency with the original scientific content. The authors take full responsibility for the final version of the figure.

CRediT Author Statement

Author Contributions: Ahmad Suseno: Writing – review & editing, Writing – original draft, Validation, Resources, Methodology, Formal analysis, Conceptualization. Kumala Nadiah Sholika: Writing – review & editing, Writing – original draft, Validation, Resources, Formal analysis, Investigation, Data curation. Yayuk Astuti: Writing – review & editing, Supervision. All authors have read and agreed to the published version of the manuscript.

References

[1] Setyono, A.E., Kiono, B.F.T. (2021). Dari energi fosil menuju energi terbarukan: potret kondisi minyak dan gas bumi Indonesia tahun 2020–2050. *Jurnal Energi Baru Dan Terbarukan*, *2*(3), 154-162. DOI: 10.14710/jebt.2021.11157.

[2] Rosmawati, R., Arita, S., Komariah, L.N., Nazarudin, N., Alfernando, O. (2019). The effect of H-USY catalyst in catalytic cracking of waste cooking oil to produce biofuel. *IJFAC (Indonesian Journal of Fundamental and Applied Chemistry)*, *4*(2), 67-71. DOI: 10.24845/ijfac.v4.i2.67.

[3] Suryatini, K.Y., Made, M.N. (2023). Pemanfaatan potensi minyak goreng bekas (jelantah) sebagai biodiesel. *Emasains: Jurnal Edukasi Matematika Dan Sains*, *12*(1), 116-124. DOI: 10.5281/zenodo.7902815.

[4] Wijaya, K., Utami, M., Damayanti, A.K., Tahir, I., Tikoalu, A.D., Rajagopal, R., Thirupathi, A., Ali, D., Alarifi, S., Chang, S.W., Ravindran, B. (2022). Nickel-modified sulfated zirconia catalyst: Synthesis and application for transforming waste cooking oil into biogasoline via a hydrocracking process. *Fuel*, *322*, 124152. DOI: 10.1016/j.fuel.2022.124152.

[5] Suseno, A. (2019, April). Hydrocracking of palm oil to gasoline on bimetallic Ni-Cu/zirconia pillared bentonite. In *IOP Conference Series: Materials Science and Engineering* (Vol. 509, No. 1, p. 012005). IOP Publishing. DOI: 10.1088/1757-899X/509/1/012005.

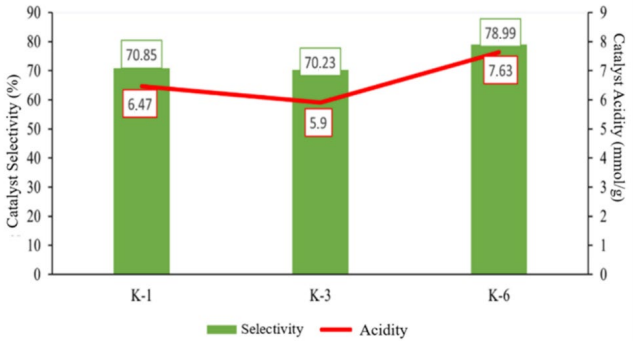


Figure 8. Correlation between catalyst acidity and selectivity.

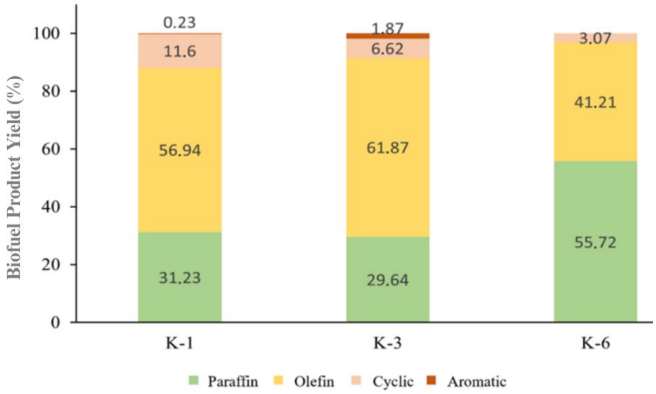


Figure 9. Percentage of biofuel product yield.

Copyright © 2027, ISSN 1978-2993

[6] Fatimah, I., Fadillah, G., Sagadevan, S., Oh, W.C., Ameta, K.L. (2023). Mesoporous silica-based catalysts for biodiesel production: a review. *ChemEngineering*, *7*(3), 56. DOI: 10.3390/chemengineering7030056.

[7] Suseno, A., Zahra, S.F., Astuti, Y., Widodo, D.S. (2025). The effect of pH on the synthesis of mesoporous silica as a carrier for the metal catalyst Ni-Cu in the hydrocracking reaction of used cooking oil into biofuel. *Cognizance Journal of Multidisciplinary Studies*, *5*(12), 23-34. DOI: 10.47760/cognizance.2025.v05i12.003.

[8] Siles-Quesada, S., Parlett, C.M., Lamb, A.C., Manayil, J.C., Liu, Y., Mensah, J., Arandiyan, H., Wilson, K., Lee, A.F. (2023). Synthesis and catalytic advantage of a hierarchical ordered macroporous KIT-6 silica. *Materials Today Chemistry*, *30*, 101574. DOI: 10.1016/j.mtchem.2023.101574.

[9] Meléndez-Ortiz, H.I., Puente-Urbina, B., Castruita-de Leon, G., Mata-Padilla, J.M., García-Uriostegui, L. (2016). Synthesis of spherical SBA-15 mesoporous silica. Influence of reaction conditions on the structural order and stability. *Ceramics International*, *42*(6), 7564-7570. DOI: 10.1016/j.ceramint.2016.01.163.

[10] Cai, S., Zhang, Y., Zhang, H., Yan, H., Lv, H., Jiang, B. (2014). Sol–gel preparation of hydrophobic silica antireflective coatings with low refractive index by base/acid two-step catalysis. *ACS Applied Materials & Interfaces*, *6*(14), 11470-11475. DOI: 10.1021/am501972y.

[11] Ahluwalia, S., Prakash, N.T., Prakash, R., Pal, B. (2016). Improved degradation of methyl orange dye using bio-co-catalyst Se nanoparticles impregnated ZnS photocatalyst under UV irradiation. *Chemical Engineering Journal*, *306*, 1041-1048. DOI: 10.1016/j.cej.2016.08.028.

[12] Suseno, A., Gunawan, G., Astuti, E.D., Wijaya, R.A. (2025). Enhanced hydrocracking of oleic acid to sustainable biofuel over Ni–Cu/mesoporous silica catalyst: Effects of reaction conditions, kinetic modelling, and mechanistic insights. *Next Materials*, *9*, 101268. DOI: 10.1016/j.nxmate.2025.101268.

[13] Das, S., Jangam, A., Du, Y., Hidajat, K., Kawi, S. (2019). Highly dispersed nickel catalysts via a facile pyrolysis generated protective carbon layer. *Chemical Communications*, *55*(43), 6074-6077. DOI: 10.1039/C9CC00783K.

[14] Wang, Y., Zhu, W., Sang, S., Gao, L., Xiao, G. (2017). Supported Cu catalysts for the hydrogenation of furfural in aqueous phase: Effect of support. *Asia-Pacific Journal of Chemical Engineering*, *12*(3), 422-431. DOI: 10.1002/apj.2085.

[15] Hasanudin, H., Asany, W.S., Syoufian, A., Wijaya, K., Mudzakir, A., Suseno, A., Rinaldi, N., Hermawan, E., Asri, W.R., Siddiqui, M.N., Saleh, T.A. (2026). Amorphous Silica Alumina Supported Nickel Sulfide Catalysts for Tunable Hydrocracking of Crude Palm Oil to Biofuel. *South African Journal of Chemical Engineering*, *57*, 100939. DOI: 10.1016/j.sajce.2026.100939.

[16] ALOthman, Z.A. (2012). A review: fundamental aspects of silicate mesoporous materials. *Materials*, *5*(12), 2874-2902. DOI: 10.3390/ma5122874.

[17] Azmiyawati, C., Setyorini, A., Muhtar, H., Sriatun, S., Darmawan, A. (2025). Optimizing nitrogen delivery: Controlled release of fertilizer using mesoporous silica for sustainable agriculture. *Particulate Science and Technology*, *43*(4), 592-602. DOI: 10.1080/02726351.2025.2478222.

[18] Isapour, G., Feng, Y., Grönbeck, H., Skoglundh, M., Härelind, H. (2026). Nature of ammonia storage sites in H-SSZ-13 and Cu-SSZ-13. *RSC Advances*, *16*(31), 28182-28190. DOI: 10.1039/D6RA03025D.

[19] Zulkepli, S., Rahman, N.A., Lee, H.V., Cheng, C.K., Chen, W.H., Juan, J.C. (2022). Synergistic effect of bimetallic Fe-Ni supported on hexagonal mesoporous silica for production of hydrocarbon-like biofuels via deoxygenation under hydrogen-free condition. *Energy Conversion and Management*, *273*, 116371. DOI: 10.1016/j.enconman.2022.116371.

[20] Widjonarko, D.M., Jumina, J., Kartini, I., Nuryono, N. (2014). Phosphonate modified silica for adsorption of Co (II), Ni (II), Cu (II), and Zn (II). *Indonesian Journal of Chemistry*, *14*(2), 143-151. DOI: 10.22146/ijc.21251.

[21] Mu, J., Liang, M., Huang, H., Meng, J., Xu, L., Song, Z., Wu, M., Miao, Z., Zhuo, S., Zhou, J. (2022). Experimental and theoretical study of ZrMo-KIT-6 solid acid catalyst with abundant Brønsted acid sites. *RSC Advances*, *12*(15), 9310-9322. DOI: 10.1039/D2RA00586G.

[22] Srinivasan, M.P., Punithavelan, N. (2018). Structural, morphological and dielectric investigations on NiO/CuO/ZnO combined semiconductor metal oxide structures based ternary nanocomposites. *Materials Research Express*, *5*(7), 075033. DOI: 10.1088/2053-1591/aad079.

[23] Anggoro, D.D., Prasetyoko, D., Hartati, H., Zakaria, Z.Y., Le Monde, B.U., Nurdiani, M. (2025). Free hydrogen-deoxygenation of waste cooking oil into green diesel over Ni-Marble waste catalyst: Optimization and economic analysis. *International Journal of Renewable Energy Development*, *14*(6), 1171-1180. DOI: 10.61435/ijred.2025.61241.

Copyright © 2027, ISSN 1978-2993

[24] Iplik, E., Aslanidou, I., Kyprianidis, K. (2020). Hydrocracking: A perspective towards digitalization. *Sustainability*, *12*(17), 7058. DOI: 10.3390/su12177058.

[25] Kang, Z., Wang, Z., Lu, Y., Cao, R., Huang, D., Meng, Q. (2022). Investigation on the effect of atmosphere on the pyrolysis behavior and oil quality of Jimusar oil shale. *Geofluids*, *2022*(1), 1408690. DOI: 10.1155/2022/1408690.

[26] Agustina, K.R.A., Subagyo, R., Jovita, S., Asikin-Mijan, N., Bahruji, H., Prasetyoko, D., Istadi, I., Widiasih, W., Habiddin, H. (2026). Selective deoxygenation of waste cooking oil to cycloparaffin over Sapindus rarak extract as templated for synthesis of Ni/Mesoporous silica catalyst. *Microporous and Mesoporous Materials*, *413*, 114278. DOI: 10.1016/j.micromeso.2026.114278..

Copyright © 2027, ISSN 1978-2993